Thermodynamics parameters for binding of halogenated benzotriazole inhibitors of human protein kinase CK2α.

Maria Winiewska, Katarzyna Kucińska, Małgorzata Makowska, Jarosław Poznański*, David Shugar*

Institute of Biochemistry and Biophysics PAS, Pawińskiego 5a, 02-106 Warszawa, Poland

*Corresponding authors: Jarosław Poznański, David Shugar, Institute of Biochemistry and Biophysics PAS, Pawińskiego 5a, 02-106 Warszawa POLAND, Tel +48 22 592 3511, Fax: +48 22 592 2190, E-mail: jarek@ibb.waw.pl, shugar@ibb.waw.pl

Abstract

The interaction of human CK2α (hCK2α) with nine halogenated benzotriazoles, **TBBt** and its analogs representing all possible patterns of halogenation on the benzene ring of benzotriazole, was studied by biophysical methods. Thermal stability of protein–ligand complexes, monitored by calorimetric (DSC) and optical (DSF) methods, showed that the increase in the mid-point temperature for unfolding of protein-ligand complexes (i.e. potency of ligand binding to hCK2α) follow the inhibitory activities determined by biochemical assays.

The dissociation constant for the ATP-hCK2α complex was estimated with the aid of Microscale Thermophoresis (MST) as 4.3±1.8 μM, and MST-derived dissociation constants determined for halogenated benzotriazoles, when converted according to known ATP concentrations, perfectly reconstruct IC_{50} values determined by the biochemical assays.

Ligand-dependent quenching of tyrosine fluorescence, together with molecular modeling and DSC-derived heats of unfolding, support the hypothesis that halogenated benzotriazoles bind in at least two alternative orientations, and those that are efficient hCK2α inhibitors bind in the orientation which **TBBt** adopts in its complex with maize CK2α.

DSC-derived apparent heat for ligand binding ($\Delta\Delta H_{bind}$) is driven by intermolecular electrostatic interactions between Lys68 and the triazole ring of the ligand, as indicated by a good correlation between $\Delta\Delta H_{bind}$ and ligand pK_a. Overall results, additionally supported by molecular modeling, confirm that a balance of hydrophobic and electrostatic interactions contribute predominantly (~40 kJ/mol), relative to possible intermolecular halogen/hydrogen bonding (less than 10 kJ/mol), in binding of halogenated benzotriazoles to the ATP-binding site of hCK2α.

Abreviations:
hCK2a – catalytic subunit of human casein kinase II;
DSC – differential scanning calorimetry;
DSF – differential scanning fluorimetry;
MST – microscale thermophoresis;
PDB – Protein Data Bank;

1. Introduction

Cellular growth and division is driven by (ir)reversible post-translational modifications (phosphorylation, glycosylation, ubiquitination, S-nitrosylation, methylation, N-acetylation, lipidation, proteolysis) and numerous nonbonding interactions with other constituents (proteins, nucleic acids, lipids, metal ions, cofactors), as well as interactions with solvent molecules [1-4]. However, specific non-covalent interactions with low-mass ligands are also of considerable importance.

Van der Waals interactions, both attractive and repulsive, are short-range interactions that control the majority of binding events [5]. Spatial compatibility directs ligand selectivity, excluding most putative ligands, and favoring those that fit to the protein binding site. Van der Waals interactions are relatively weak (0.1- 4 kJ/mol), when compared to other non-covalent interactions, albeit the large number of contacts created upon molecular recognition makes their contribution to the Gibbs' free energy of interaction significant, the maximum of which is attained when the shapes of ligand and protein binding site are complementary. This corresponds to the Lock and Key analogy originally postulated in 1894 by Emil Fischer, and further extended to the Induced-Fit Theory, describing dynamic changes of protein structure upon ligand binding (see [6] for review). Basically, binding events occur when they are accompanied by a decrease of Gibbs' free energy of binding (ΔG), resulting from a balance between entropic ($-T\Delta S$) and enthalpic (ΔH) components. It should be stressed that notwithstanding direct protein-ligand interactions, solvent molecules, surrounding both in free and bound states, may also contribute substantially to changes of these thermodynamic parameters. Other medium- and long-range interactions are generally associated with electron densities distributed on the interacting species. The strongest occur between charged groups, known as salt-bridges [7], the contribution of which, to the Gibbs' free energy, approaches 40 kJ/mol [8]. The next terms describe charge-dipole, dipole-dipole and higher-order interactions, which decrease more rapidly with the distance between components.

Hydrogen bonds contribute significantly to the organization of intermolecular complexes. The energy of a single hydrogen bond (H-bond) in protein-ligand complexes depends both on the type of hydrogen bond donor (D) and acceptor (A) pairs, and on the overall geometry of the D-H···A system [9], varying in a range of 5 to 20 kJ/mol. Subsequently, numerous non-canonical weak H-bonds have been identified by statistical analyses of protein structures, including a π-electron system acting as an H-bond acceptor [10-12], and an aliphatic carbon acting as an H-bond donor [11, 13-15].

During the past decade, halogen bonding (X-bond, see [16] for review) has been identified as an alternative to H-bonding in many crystal structures of low-mass ligands and their possible supramolecular ensembles [16-27], as well as in complexes of biomolecules with halogenated ligands [28-30]. The role of halogenated ligands in biological systems has been

widely reviewed, amongst others, by Auffinger *et al.* [28], Parisini *et al.* [31], Rendine *et al.* [30], Voth & Ho [32], Voth *et al.* [33], Scholfield *et al*. [34], Wilcken *et al.* [35] and Poznański & Shugar [36]. However, the thermodynamic contribution of a halogen bond is still under debate [27, 32, 37-47], estimates of which vary from 0.8 [44] up to 30 kJ/mol [32]. Numerous natural drugs and an increasing number of synthetic drug candidates are halogenated [48-50], and comprise almost 20% of low-mass protein ligands accessible in the Protein Data Bank (PDB) [47]. Consequently, understanding the thermodynamics of ligand binding, including the possible contribution of halogen bonding, should support rational drug design of halogenated compounds.

Protein kinase CK2 was selected as a model protein. It is a constitutively active Ser/Thr protein kinase that regulates hundreds of independent cellular processes - more than 300 protein substrates have been identified [51]. CK2 has become a therapeutic target for inhibitors directed to cancer treatment [52, 53] because of the strong correlation between malignancy and an abnormally high activity of CK2 in cancer cells [54]. An increasing number of high-resolution structures of CK2-ligand complexes help in the *in-silico* development of new CK2 inhibitors [55] - many of them halogenated.

4,5,6,7-tetrabromo-1H-benzotriazole (**TBBt**, Scheme 1) is an ATP-competitive inhibitor displaying reasonable selectivity for CK2 and its catalytic subunit CK2α [52, 53], which target the ATP-binding site [56, 57]. More potent inhibitors have since been reported, many of them designed as **TBBt** analogues [58, 59].

Analysis of a series of nine benzotriazoles brominated on the benzene ring clearly showed that their inhibitory activity against CK2α is strongly correlated with their physico-chemical properties (aqueous solubility, molecular volume, pK_a for dissociation of the triazole proton) [60, 61]. We have also shown that a balance of hydrophobic and electrostatic interactions, with an eventual possible contribution of halogen bonding, drive inhibitory activities of benzotriazoles halogenated on the benzene ring [60-63].

There are numerous data concerning individual ligands, but only few reports concerning screening tests for binding of low-mass ligands by protein kinases [64-70]. And only limited data concern systematic thermodynamic studies on a series of closely related substrate-mimicking peptides [71-73] or low-mass ligands [74, 75]. Herein, we analyze the activity of **TBBt** and some close analogues, in which selected bromine atoms are replaced by hydrogen, in terms of thermodynamic parameters describing protein-ligand interactions obtained by optical (differential scanning fluorimetry, DSF) and calorimetric (differential scanning calorimetry, DSC) methods. Stability constants for the seven most potent ligands were additionally estimated at 25 °C by Microscale Thermophoresis (MST).

2. Materials and Methods

2.1. Synthetic Procedures

All reagents and solvents were purchased from Sigma Aldrich, Chempur, Avantor and Merck. Thin-layer chromatography (TLC) was performed on 0.2 mm Merck silica gel 60 F254 plates, and column chromatography with Merck silica gel 60 (230 – 400 mesh).

All brominated ligands (Scheme 1) were prepared according to previously reported procedures [60, 62]. ^{13}C NMR and Mass spectra for the final compounds are consistent with those reported originally [60, 62]. In some cases the procedures were further optimized (see Supplementary Materials for details).

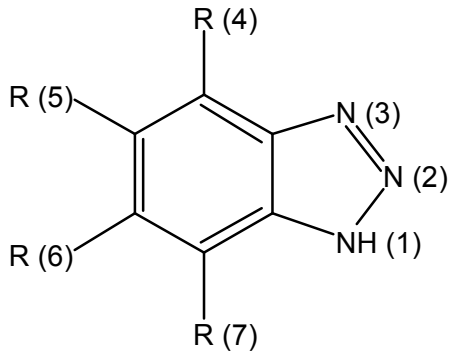

4-BrBt	R(4) - Br; R(5), R(6), R(7) - H
5-BrBt	R(5) - Br; R(4), R(6), R(7) - H
4,5-Br_2Bt	R(4), R(5) - Br; R(6), R(7) - H
4,6-Br_2Bt	R(4), R(6) - Br; R(5), R(7) - H
4,7-Br_2Bt	R(4), R(7) - Br; R(5), R(6) - H
5,6-Br_2Bt	R(5), R(6) - Br; R(4), R(7) - H
4,5,6-Br_3Bt	R(4), R(5), R(6) - Br; R(7) - H
4,5,7-Br_3Bt	R(4), R(5), R(7) - Br; R(5) - H
TBBt	R(4), R(5), R(6), R(7) - Br

Scheme 1. All possible benzotriazole derivatives halogenated on the benzene ring

4-bromo-1H-benzotriazole (**4-BrBt**) was obtained from 2,1,3-benzothiadiazole by selective bromination [79], followed by reductive sulfur extrusion [81] and diazotization with $NaNO_2$ [63].

5-Bromo-1H-benzotriazole (**5-BrBt**) was prepared from 4-bromo-*o*-phenylenediamine by diazotization with $NaNO_2$ [63].

4,5-Dibromo-1H-benzotriazole (**4,5-Br_2Bt**) was prepared by bromination of commercially available 5-bromo-2,1,3-benzothiadiazole [79], followed by reductive sulfur extrusion [81] and diazotization [63].

4,6-Dibromo-1H-benzotriazole (**4,6-Br_2Bt**) was prepared by reduction of 2,4-dibromo-6-nitroaniline with $SnCl_2$ [63]. The crude 3,5-dibromo-*o*-phenylenediamine dihydrochloride was then reacted with $NaNO_2$ to give the desired product [63].

4,7-dibromo-1H-benzotriazole (**4,7-Br_2Bt**). Selective bromination of 2,1,3-benzothiadiazole [79] obtained from commercially available *o*-phenylenodiamine [80], followed by reductive sulfur extrusion [81] and diazotization with $NaNO_2$ [63] gave the desired product.

5,6-Dibromo-1H-benzotriazole (**5,6-Br_2Bt**) was prepared by bromination of *o*-phenylenediamine (amine groups protected with *p*-toluenesulphonyl chloride [77]) followed by deprotection with concentrated H_2SO_4 and diazotization with $NaNO_2$ [63].

4,5,6-Tribromo-1H-benzotriazole (**4,5,6-Br$_3$Bt**). Nitration of commercially available 1,2,3-tribromo-5-nitrobenzene [60], followed by reduction and diazotization [63], gave the desired product.

4,5,7-Tribromo-1H-benzotriazole (**4,5,7-Br$_3$Bt**). After bromination of commercially available 5-methyl-1*H*-benzotriazole [78], the methyl group was oxidized with $KMnO_4$, and the carboxyl group was removed by reaction with quinoline [62].

4,5,6,7-Tetrabromo-1H-benzotriazole (**TBBt**) was prepared from 1*H*-benzotriazole [76].

2.2. Expression and purification of hCK2α

Plasmid pET28 containing DNA encoding human CK2α subunit (kindly provided by the Laboratory of RNA Biology and Functional Genomics IBB PAN) was transformed into BL21(DE3) *E. coli* cells. A single colony was inoculated in 30 ml LB broth supplemented with kanamycin (50 μg/ml) and incubated overnight at 37 ºC. The culture (5 ml) was used to inoculate 1000 ml of Luria Broth with kanamycin (50 μg/ml) and cells were cultured at 37 °C until OD_{600} reached 0.5, when hCK2α expression was induced by 0.5 mM Isopropylthio-β-galactoside. Cells were then incubated at 37 ºC for 4 hours, harvested by centrifugation at 6000 rpm for 10 min at 4 ºC, and stored at -20 ºC.

Thawed cells were suspended in 30 ml of buffer A (25 mM Tris-HCl pH 8, 500 mM NaCl, 10 mM imidazole, 5 mM β-mercaptoethanol) with 0.2 mM PMSF (phenylmethylsulfonyl fluoride) and protease inhibitor cocktail (Sigma-Aldrich P8849), and sonicated by five 1-min bursts. The cell lysate was centrifuged at 20000 rpm for 40 min, and the supernatant fraction processed by Ni^{2+}-NTA agarose chromatography under non-denaturing conditions. The protein was then purified by affinity chromatography with a HiTrap Heparin HP column (GE HealthCare), and eluted with a linear 0.4 to 1 M NaCl gradient buffered with 25 mM Tris-HCl, pH 8.5. Purified $(His)_6$-tagged hCK2α was concentrated by ultrafiltration, rebuffered in 500 mM NaCl, 50% glycerol, 1 mM DTT, 25 mM Tris-HCl, pH 8.5, and stored at -80 °C. The final yield of purified protein was 20 mg/l. Concentration of purified protein was estimated by UV absorbance at 280 nm, assuming a molar extinction coefficient $\varepsilon = 61895\ M^{-1}cm^{-1}$. Protein purity was further checked by sodium dodecyl sulfate polyacrylamide gel electrophoresis.

2.3. Sample preparation.

In all experiments hCK2α was diluted with 25 mM Tris-HCl (pH 8, 0.5 M NaCl) to the required protein concentration. In fluorescence and MST experiments the buffer contained additionally 5 mM β-mercapthoethanol.

All ligands were initially dissolved in dimethyl sulfoxide (DMSO), and the appropriate amounts of ligand stock solutions were diluted with DMSO prior to addition to the protein samples to obtain the required ligand concentration with a final DMSO concentration of 2%.

2.4. Molecular Modeling of the complex of TBBt with human CK2α.

The ensemble of seven structures was modeled by homology, based on the highest-resolution structures of human CK2α found in the Protein Data Bank (PDB: 3at2 [82], 3bqc [83], 3h30 [84], 3nsz [85], 3pe1 [86], 3war [87], 4kwp [88]). Each was then structurally aligned with the complex of **TBBt** with maize CK2α (PDB: 1j91 [57]), using the Mustang algorithm [89] implemented in the Yasara Structure Package [90]. The location of the **TBBt** ligand was then adopted directly from its complex with maize CK2α, and the resulting structures of the complex were tuned by 1 ns Molecular Dynamics with all residues located outside a 10 Å sphere centered at **TBBt** kept fixed. Alternative binding orientations for **TBBt** were analogously adopted (without MD-tuning) from the complexes of maize CK2α with *4,5,6,7-tetrabromo-1H-benzimidazole* (PDB: 2oxy [91]) and *3,4,5,6,7-pentabromo-1H-indazole* (PDB: 3kxg [53]), which are the closest structural analogues of **TBBt**.

2.5. Differential scanning fluorimetry (DSF)

Fluorescence data were collected on a Varian Cary Eclipse spectrofluorometer, equipped with a constant-temperature cell holder, using 10-mm path-length cuvettes. Protein emission was monitored at 335 nm (excitation at 280 nm) at temperatures of 20 to 80 ºC, with 1 ºC/min heating rate. The protein (hCK2α) was diluted to a final concentration of 0.25 μM (see Section 2.3).

All the numerical models were individually fitted to experimental data, assuming a two-state cooperative transition at T_m, using the Marquardt algorithm [92] implemented in the GnuPlot program [93] according to Equation 1.

$$I(T) = \frac{I_U(T) + I_F(T) \cdot e^{(T_m - T) \cdot p}}{1 + e^{(T_m - T) \cdot p}} \quad (1)$$

where p mimics the slope of I(T) at T_m, and $I_F(T)$ and $I_U(T)$ are linear approximates of the temperature-dependence of fluorescence intensities of the folded (F) and unfolded (U) states, respectively. The final results (see Table 1) are weighted-averages from at least 5 independent experiments.

2.6. Differential scanning calorimetry (DSC)

All measurements were carried on a Nano DSC differential scanning calorimeter (TA Instruments) equipped with cells of 300 μL volume (both sample and reference). A pressure of 3 atm was applied to prevent solvent vaporization upon heating. Protein thermal denaturation was followed by the heat flow accompanying variations in the sample heat capacity. The temperature was varied in the range 20-80 ºC (scan rate of 1 ºC/min). The protein concentration was 0.25 mg/ml (5.43 μM), and appropriate DMSO solutions of ligands were added to obtain a 1:1 ligand to protein molar ratio with a final DMSO concentration of 2% (v:v). All experiments were repeated at least 2 times. Base-line correction, heat effect determined by peak integration, and estimates of temperature of unfolding (T_m) were done

using the NanoAnalyze Data Analysis software (TA instruments). Further extrapolations of ΔG to 25 ºC were done according to Equation 2 [94]:

$$\begin{aligned}
&\Delta H(T_m) = \Delta H_{cal} \\
&\Delta S(T_m) = \Delta H(T_m)/T_m \\
&\Delta H(T) = \Delta H(T_m) + \Delta C_p \cdot (T - T_m) \\
&\Delta S(T) = \Delta S(T_m) + \Delta C_p \cdot \ln(T/T_m) \\
&\Delta G(T) = \Delta H(T) - T \cdot \Delta S(T)
\end{aligned} \tag{2}$$

where a change in the heat capacity upon unfolding (ΔCp) was assumed temperature-independent, and the value of which, at T_m, was roughly estimated from heat-flow thermograms as the difference between high- and low-temperature asymptotes at T_m. Entropy, enthalpy and free energy for ligand binding were then calculated as the difference between appropriate thermodynamic parameters estimated separately for free and ligand-bound protein.

2.7. Microscale thermophoresis (MST)

The hCK2α was initially labeled with the commercially available NT-647 dye, using NanoTemper's Protein Labeling Kit RED. The concentration of labeled protein was kept constant at ~100 nM. The ligand to protein concentration ratio was tested in the range of 0.01 to 100. Samples were loaded into K002 Monolith™ NT.115 Standard Treated Capillaries. After a short incubation period, MST analysis was performed using the Monolith NT.115 (NanoTemper Technologies). All numerical models were fitted to experimental data using the NT Analysis 1.5.41 software (NanoTemper Technologies). Presented results are weighted-averages of at least 5 independent experiments.

MST-derived K_{diss} values were converted to inhibitory activities, assuming competition between the halogenated ligand and ATP, according to Equation 3 [95]:

$$IC_{50} = K_{diss,ligand} \cdot \left(1 + \frac{[ATP_{tot}]}{K_{diss,ATP}}\right) \tag{3}$$

3. Results

3.1. Fluorescence-monitored melting of hCK2α complexes (DSF).

Inspection of the ensemble of complexes of human CK2α with **TBBt**, which were modeled by homology on the basis of **TBBt** bound to maize CK2α (PDB: 1j91) clearly indicates that Tyr50 is the major sensor for binding at the ATP-binding site of **TBBt** and its homologues, since its fluorescence may be quenched directly by the ligand located within a distance of 7-9 Å (see Figure 1). The distance of the ligand located at the ATP-binding site from the remaining Tyrosine residues exceeds 12.5 Å, so that ligand-induced changes in their fluorescence are negligible. Moreover, the next two closest tyrosine residues (Tyr39 and

Tyr125) are shielded from the ligand by electron densities of the β-sheets that border the ATP-binding site.

Figure 1.

The changes in the distance and orientation of the Tyr50 phenol ring relative to the ligand strongly depend on the spatial organization of the glycine-rich loop, the conformation of which is highly diversified in accessible structures of CK2α [96], and on the location of the ligand at the ATP-binding site, which also varies in complexes with protein kinases [36]. This structural flexibility renders Tyr50 sensitive, not only to the population of the bound ligand, but also to any changes in its orientation and/or its ionic state.

Thermal stability of hCK2α and its 1:1 and 10:1 complexes (ligand to protein concentration ratio) with all nine halogenated benzotriazoles was studied with the aid of fluorescence-monitored thermal denaturation. The ATP-bound form of the protein was tested as the reference. None of the ligands interact with an unfolded form of hCK2α, as indicated by a common trend of temperature-dependence of fluorescence intensity observed for the high-temperature region (T > 60 °C in Figure 2).

Inspection of the denaturation curves shows that the nine ligands cluster into three groups (see Fig. 2A, B). At 20 °C, when the protein is folded, four of them, namely **TBBt**, **4,5,6-Br$_3$Bt, 5,6-Br$_2$Bt** and **5-BrBt**, strongly quench tyrosine fluorescence, even at a 1:1 protein to ligand ratio (Figure 2A). The mid-point temperature of complexes with these ligands, T_m, is also increased (Table 1, Figure 2D), indicating that all of them bind efficiently to hCK2α at submicromolar concentrations, and the structure of the protein is visibly stabilized when each of these ligands is bound. All ligands, with the exception of **5-BrBt**, carry two bromine atoms at C(5)/C(6) of the benzene ring of benzotriazole (see Scheme 1). Since all these ligands similarly quench tyrosine fluorescence, it might be deduced that each of them binds to hCK2α in an almost identical orientation, putatively close to that at which **TBBt** is found in the crystal structure of maize CK2α (PDB: 1j91) [57], or modeled in the complex with human CK2α (Figure 1).

The next three ligands, **4,5,7-Br$_3$Bt, 4,6-Br$_2$Bt and 4,5-Br$_2$Bt**, also visibly shift T_m, but to a lesser extent than for the first group of ligands. Moreover, they affect tyrosine fluorescence only at higher ligand excess (Figure 2B), and the observed tyrosine fluorescence quenching is weaker than that for **TBBt**. Both effects indicate that all three bind to hCK2α more weakly than any from the previous group. An analogous trend in fluorescence quenching has been recently observed for **TBBt** and **TBBz**, which bind to maize CK2α in different orientations (see structures based on PDB: 1j91 [57] and PDB: 2oxy [91] in Figures 6A and 6B, respectively), and also for their derivatives with bromine at C4 replaced by a methyl group [63]. It may thus be hypothesized that **4,5-Br$_2$Bt, 4,6-Br$_2$Bt**, and most likely **4,5,7-Br$_3$Bt**, bind to CK2α in different orientations than **TBBt**. All these ligands carry only a single bromine atom at C(5)/C(6).

Finally, in the entire range of scanned temperatures, virtually no changes in fluorescence are observed for ligands halogenated solely at sites proximal to the triazole ring, C(4) and/or C(7): **4,7-Br$_2$Bt** and **4-BrBt**. This indicates that these two compounds virtually do not interact with hCK2α.

Figure 2.

Contrary to the strongly binding halogenated benzotriazoles (**TBBt**, **4,5,6-Br$_3$Bt, 5,6-Br$_2$Bt** and **5-BrBt)**, ATP only minimally changes the fluorescence of the folded form of hCK2α, albeit at a higher concentration of 2.5 μM it increases thermal stability of the protein by ~2 °C (Figure 2C).

The observed ATP-induced increase in the thermal stability of hCK2α shows that all ligands that shift unfolding temperature by less than 2 °C cannot compete with ATP, and thus cannot be regarded as putative CK2α inhibitors. In this context, only the first group of halogenated benzotriazoles (**TBBt**, **4,5,6-Br$_3$Bt, 5,6-Br$_2$Bt** and **5-BrBt**) may be considered as potential inhibitors.

3.2. Differential Scanning Calorimetry (DSC)

DSC was applied to monitor thermal denaturation of free hCK2α and its nine 1:1 complexes with halogenated benzotriazoles. After correction for the low- and high-temperature asymptotes, the two thermodynamic parameters could be estimated directly from the thermograms: T_m as the location of the maximum, and ΔH_{cal} as the area under the heat-flow curve (Figure 3A). As expected, all these temperatures agree with the DSF-derived temperatures for denaturation of the ligand-protein complexes (Figure 3B). The change in heat capacity associated with protein unfolding (ΔCp) was roughly estimated as the difference between the low- and high-temperature heat-flow asymptotes at T_m. The resulting thermodynamic parameters are presented in Table 1.

Figure 3.

All complexes with ligands carrying at least one bromine at C(5)/C(6) are much more stable (i.e. display higher T_m and ΔG_{unf} values) than free hCK2α. And the higher the T_m with a given ligand, the more efficiently it binds, as indicated by the values of ΔG_{bind} and K_{diss} extrapolated to 25 °C. Unfortunately, extrapolation of the other thermodynamic parameters related to ligand binding are heavily biased, due to possible temperature-dependence of ΔCp (see Equation 2). Predominance of the heat of protein unfolding (H_{unf}) over the heat of binding of small ligands ($\Delta H_{bind} = -\Delta H_{diss}$) precludes reliable estimates of heat of binding. Moreover, the contribution of the temperature-dependent entropy of hydration for a highly hydrophobic ligand to the Free Gibbs Energy of binding, estimated from DSC, may also significantly contribute to lowering of the apparent DSC-derived dissociation constants. However, the relation between ligand-induced changes in the unfolding temperature (T_m) and the apparent heat of ligand dissociation at T_m ($\Delta\Delta H_{cal} = \Delta H_{cal} - \Delta H_{cal,apo}$) clearly shows that the enthalpic contribution to the free energy of binding for the four most potent ligands

(**TBBt**, **4,5,6-Br$_3$Bt, 5,6-Br$_2$Bt** and **5-BrBt**) is visibly larger than that for the other ligands (Figure 4A), and a positive correlation between $\Delta\Delta H_{cal}$ and ΔT_m points, at least at 50 °C, to a favorable enthalpic contribution to the free energy of binding. Moreover, the heat of dissociation for **TBBt**, **4,5,6-Br$_3$Bt, 5,6-Br$_2$Bt** and **5-BrBt** clearly decreases when the pK_a of the ligand increases, while for the others the changes are much more moderate (Figure 4B). This agrees with the observed preference of CK2α for hydrophobic anions [91].

Figure 4.

The foregoing, together with the variations in quenching of tyrosine fluorescence (Figure 2), and molecular modeling (Figure 1), support binding of **TBBt**, **4,5,6-Br$_3$Bt, 5,6-Br$_2$Bt** and **5-BrBt** to hCK2α at the ATP-binding site in an orientation that enables short-range electrostatic interactions between the triazole ring of ligand and a proximal side-chain of Lys68 (Figure 5A). Other orientations of the ligand, some of which are shown in Figures 5B and 5C, preclude efficient electrostatic interactions, resulting in a substantial decrease of the heat of ligand binding and, in parallel, the heat effect is less sensitive to ligand electronic properties. This agrees with the data for **4-BrBt, 4,5-Br$_2$Bt, 4,6-Br$_2$Bt, 4,7-Br$_2$Bt** and **4,5,7-Br$_3$Bt**, the heat of dissociation for which does not depend on their pK_a, and the value of ~50 kJ/mol may reflect the enthalpic effect of a release of some water molecules upon ligand binding. Since the enthalpy of formation of an individual hydrogen bond in bulk water has been estimated as 15 kJ/mol [97], the observed gain of 50-75 kJ/mol corresponds to possible formation of additional 3-5 hydrogen bonds involving water molecules released to bulk solvent upon ligand binding.

Figure 5.

3.3. Microscale Thermophoresis (MST)

MST, like Isothermal Titration Calorimetry (ITC), also supports determination of binding affinities at constant temperature, albeit both methods substantially differ in the required sample concentrations. Another advantage of MST is the relatively small sample consumption of measurements carried out in microcapilaries, but the protocol of sample preparation implies a short preincubation of protein-ligand solutions. The MST method was used to verify results obtained by temperature-scanning methods, and permitted direct determination at 25 °C of binding affinities for the seven most potent ligands (see Figure 6 and Table 1).

Figure 6.

The order of the estimated dissociation constants (K_{diss}) determined by MST agrees with DSC-derived data extrapolated to 25 °C, but the latter values are systematically overestimated. This is most probably due to an eventual uncontrolled temperature-dependence of ΔCp, the contribution of which may differ substantially for each ligand. However, together they tend to compensate, resulting in the general trend presented in Figure 7A.

Figure 7.

MST-derived dissociation constants were also converted to IC_{50} data according to Equation 3, using $[ATP_{tot}]$ = 10 μM [61] and measured K_{diss} for ATP of 4.3±1.8 μM. The MST-derived IC_{50} values are in full accord with inhibitory activities determined by biochemical assay [61]. It should however be noted that MST-derived dissociation constants may be slightly underestimated due to possible non-specific ligand binding, which was occasionally observed at high excess of ligand.

4. Discussion

Comparison of binding affinities obtained by different methods shows that, despite some discrepancies between methods, the ordering of ligands based on their potency of binding is consistent with their inhibitory activities (see Figures 7B, 8A and 8B). It follows that DSF measurements with a 10-fold ligand excess, followed by DSC analysis of 1:1 complexes, recently suggested to be optimal in drug screening [75, 98], effectively screens for efficient CK2α inhibitors. However, MST results may be used alternatively to the biochemical assay [99], as shown in Figure 7B.

Figure 8.

The systematic deviations observed for **5-BrBt** must be assigned directly to the difference in the experimental setups of thermodynamics (pH = 8) and biochemical (pH = 7.5) approaches, while **5-BrBt** at pH 7 binds substantially weaker. This difference in solvent pH is critical for the ionic state of this ligand, the pK_a for which equals 7.55. This discrepancy points again to predominance of electrostatic interactions in binding of **TBBt** derivatives at the ATP-binding site of CK2α.

MST-derived binding affinities of halogenated benzotriazoles are correlated with their aqueous solubility. This implies that ligand-solvent interactions are the driving force contributing to the apparent free energy of ligand-protein interactions. The observed three general "partial"-correlation lines must be the result of substantial differences in protein-ligand interactions with an eventual contribution of ligand-ligand interactions in the solid-state. The systematic decrease of binding affinities observed for **4-BrBt**, **4,5-Br_2Bt**, **4,6-Br_2Bt**, **4,7-Br_2Bt** should be assigned to variation in electrostatic interactions between the dissociated triazole ring of the ligand and the side-chain of Lys68 that arise from the different locations of these ligands at the ATP-binding site (Figure 5) deduced from DSF and DSC data. The observed difference of approximately 20 kJ/mol (large arrow in Figure 9) is in accord with the reported contribution of individual salt-bridges to the Gibbs' free energy [8]. The internal variance in strongly binding ligands of ~10 kJ/mol (**TBBt**, **4,5,6-Br_3Bt, 5,6-Br_2Bt, 5-BrBt,** and most likely **4,5,7-Br_3Bt**) must consequently be attributed to other types of specific ligand-protein interactions, including the eventual contribution of halogen bonding observed in the crystal structure of **TBBt** bound to maize CK2α [36].

Figure 9.

Acknowledgements.

This work was supported by the Polish National Centre for Science grant 2012/07/B/ST4/01334. The equipment used was sponsored in part by the Centre for Preclinical Research and Technology (CePT), a project co-sponsored by European Regional Development Fund and Innovative Economy, The National Cohesion Strategy of Poland.

Figure captions:

Figure 1. Orthogonal views demonstrating location of Tyrosine residues proximal to **TBBt** bound at the ATP-binding site of human CK2α. Tyr50, which should be the most sensitive to ligand binding, is denoted by a black arrow, while **TBBt** is represented by vdW spheres. The ensemble of structures was modeled by homology, based on the reported structure of **TBBt** bound to maize CK2α (PDB: 1j91 [57]) and the highest-resolution structures of human CK2α (PDB: 3at2 [82], 3bqc [83], 3h30 [84], 3nsz [85], 3pe1 [86], 3war [87], 4kwp [88]).

Figure 2. Impact of binding of halogenated benzotriazoles on the thermal stability of hCK2α monitored by tyrosine fluorescence for 1:1 (A) and 10:1 (B) ligand to protein ligand ratios. As the reference the effect of ATP at 1:1 and 10:1 excess on the CK2α thermal stability is presented (C, empty and solid squares, respectively). The unfolding temperatures (D) were estimated for each ligand at 1:1 (black diamonds) and 10:1 (open diamonds) concentration ratios according to Equation 1.

Figure 3. DSC heat-flow thermograms for hCK2α and its 1:1 complexes with halogenated benzotriazoles (A), and the comparison of DSC-derived temperatures of thermal unfolding with those determined using DSF (B).

Figure 4. Relation between DSC-derived heat for dissociation ($\Delta\Delta H_{cal}$) and (A) shift in the temperature of thermal denaturation (ΔT_m), and (B) pK_a for dissociation of the free ligand in aqueous medium (B).

Figure 5. View of the possible orientations of TBBt-like ligand at the ATP binding site of hCK2α, locations of which were adopted from known structures of the complexes of maize CK2α with **TBBt** (A), *4,5,6,7-tetrabromo-1H-benzimidazole* (B) and *3,4,5,6,7-pentabromo-1H-indazole* (C), which are the closest structural analogues of **TBBt**. Side-chains of Lys68 and Asp175, which are responsible for electrostatic interactions with the ligand, together with Tyr50, which senses ligand binding, are represented in sticks model.

Figure 6. MSC-derived pseudotitration data for binding of halogenated benzotriazoles to hCK2α.

Figure 7. Correlation between dissociation constants, K_{diss}, determined for the binding of halogenated benzotriazoles to hCK2α, using MST with DSC-derived data extrapolated to 25 °C (A). The inhibitory activities predicted from MST data according to equation 3 are compared with previously determined IC_{50} data (B).

Figure 8. Ordering of nine halogenated benzotriazoles by their strength of binding to hCK2α compared with the IC_{50} data for DSF-derived mid-point temperatures (A) and DSC-derived dissociation constants (B).

Figure 9. Relation between DSC-derived free energy for binding of halogenated ligands to hCK2α and their solubility in aqueous medium.

References:

[1] R. Lumry, S. Rajender, Enthalpy-entropy compensation phenomena in water solutions of proteins and small molecules - a ubiquitous property of water, Biopolymers, 9 (1970) 1125-1227.

[2] S.N. Timasheff, The control of protein stability and association by weak-interactions with water - how do solvents affect these processes, Annual Review of Biophysics and Biomolecular Structure, 22 (1993) 67-97.

[3] P.W. Fenimore, H. Frauenfelder, B.H. McMahon, F.G. Parak, Slaving: Solvent fluctuations dominate protein dynamics and functions, Proceedings of the National Academy of Sciences of the United States of America, 99 (2002) 16047-16051.

[4] Y. Levy, J.N. Onuchic, Water mediation in protein folding and molecular recognition, Annual Review of Biophysics and Biomolecular Structure 2006, pp. 389-415.

[5] E. Barratt, R.J. Bingham, D.J. Warner, C.A. Laughton, S.E.V. Phillips, S.W. Homans, Van der waals interactions dominate ligand-protein association in a protein binding site occluded from solvent water, Journal of the American Chemical Society, 127 (2005) 11827-11834.

[6] D.E. Koshland, The key-lock theory and the induced fit theory, Angewandte Chemie-International Edition, 33 (1994) 2375-2378.

[7] O. Keskin, B.Y. Ma, R. Nussinov, Hot regions in protein-protein interactions: The organization and contribution of structurally conserved hot spot residues, Journal of Molecular Biology, 345 (2005) 1281-1294.

[8] Z.S. Hendsch, B. Tidor, Do salt bridges stabilize proteins? A continuum electrostatic analysis, Protein Science, 3 (1994) 211-226.

[9] L. Stryer, Biochemistry (4th edition), W. H. Freeman & Company1995.

[10] J.L. Atwood, F. Hamada, K.D. Robinson, G.W. Orr, R.L. Vincent, X-ray diffraction evidence for aromatic π hydrogen-bonding to water, Nature, 349 (1991) 683-684.

[11] C.B. Aakeroy, K.R. Seddon, The hydrogen-bond and crystal engineering, Chemical Society Reviews, 22 (1993) 397-407.

[12] T. Steiner, G. Koellner, Hydrogen bonds with π-acceptors in proteins: Frequencies and role in stabilizing local 3D structures, Journal of Molecular Biology, 305 (2001) 535-557.

[13] R. Taylor, O. Kennard, Crystallographic evidence for the existence of C-H···O, C-H···N, and C-H···C hydrogen-bonds, Journal of the American Chemical Society, 104 (1982) 5063-5070.

[14] G.R. Desiraju, The C-H···O hydrogen-bond in crystals - what it is, Accounts of Chemical Research, 24 (1991) 290-296.

[15] G.R. Desiraju, The C-H···O hydrogen bond: Structural implications and supramolecular design, Accounts of Chemical Research, 29 (1996) 441-449.

[16] P. Metrangolo, F. Meyer, T. Pilati, G. Resnati, G. Terraneo, Halogen bonding in supramolecular chemistry, Angewandte Chemie-International Edition, 47 (2008) 6114-6127.
[17] O. Hassel, J. Hvoslef, The structure of bromine 1,4-dioxanate, Acta Chemica Scandinavica, 8 (1954) 873-873.
[18] H.A. Bent, Structural chemistry of donor-acceptor interactions, Chemical Rewievs, 68 (1968) 587-648.
[19] G.R. Desiraju, Supramolecular synthons in crystal engineering - a new organic-synthesis, Angewandte Chemie-International Edition in English, 34 (1995) 2311-2327.
[20] P. Metrangolo, G. Resnati, Halogen bonding: A paradigm in supramolecular chemistry, Chemistry-a European Journal, 7 (2001) 2511-2519.
[21] P. Metrangolo, H. Neukirch, T. Pilati, G. Resnati, Halogen bonding based recognition processes: A world parallel to hydrogen bonding, Accounts of Chemical Research, 38 (2005) 386-395.
[22] K. Rissanen, Halogen bonded supramolecular complexes and networks, CrystEngComm, 10 (2008) 1107-1113.
[23] C.B. Aakeroy, N.R. Champness, C. Janiak, Recent advances in crystal engineering, CrystEngComm, 12 (2010) 22-43.
[24] T.J. Mooibroek, P. Gamez, Halogen ··· phenyl supramolecular interactions in the solid state: hydrogen versus halogen bonding and directionality, CrystEngComm, 15 (2013) 1802-1805.
[25] T.J. Mooibroek, P. Gamez, Halogen bonding versus hydrogen bonding: what does the Cambridge Database reveal?, CrystEngComm, 15 (2013) 4565-4570.
[26] A. Mukherjee, S. Tothadi, G.R. Desiraju, Halogen Bonds in Crystal Engineering: Like Hydrogen Bonds yet Different, Accounts of Chemical Research, 47 (2014) 2514-2524.
[27] C.B. Aakeroey, S. Panikkattu, P.D. Chopade, J. Desper, Competing hydrogen-bond and halogen-bond donors in crystal engineering, Crystengcomm, 15 (2013) 3125-3136.
[28] P. Auffinger, F.A. Hays, E. Westhof, P.S. Ho, Halogen bonds in biological molecules, Proceedings of the National Academy of Sciences of the United States of America, 101 (2004) 16789-16794.
[29] A.R. Voth, P.S. Ho, The role of halogen bonding in inhibitor recognition and binding by protein kinases, Current Topics in Medicinal Chemistry, 7 (2007) 1336-1348.
[30] S. Rendine, S. Pieraccini, A. Forni, M. Sironi, Halogen bonding in ligand-receptor systems in the framework of classical force fields, Physical Chemistry Chemical Physics, 13 (2011) 19508-19516.
[31] E. Parisini, P. Metrangolo, T. Pilati, G. Resnati, G. Terraneo, Halogen bonding in halocarbon-protein complexes: a structural survey, Chemical Society Reviews, 40 (2011) 2267-2278.
[32] A.R. Voth, F.A. Hays, P.S. Ho, Directing macromolecular conformation through halogen bonds, Proceedings of the National Academy of Sciences of the United States of America, 104 (2007) 6188-6193.
[33] A.R. Voth, P. Khuu, K. Oishi, P.S. Ho, Halogen bonds as orthogonal molecular interactions to hydrogen bonds, Nature Chemistry, 1 (2009) 74-79.
[34] M.R. Scholfield, C.M. Vander Zanden, M. Carter, P.S. Ho, Halogen bonding (X-bonding): A biological perspective, Protein Science, 22 (2013) 139-152.
[35] R. Wilcken, M.O. Zimmermann, A. Lange, A.C. Joerger, F.M. Boeckler, Principles and Applications of Halogen Bonding in Medicinal Chemistry and Chemical Biology, Journal of Medicinal Chemistry, 56 (2013) 1363-1388.
[36] J. Poznanski, D. Shugar, Halogen bonding at the ATP binding site of protein kinases: Preferred geometry and topology of ligand binding, Biochimica Et Biophysica Acta-Proteins and Proteomics, 1834 (2013) 1381-1386.
[37] R.G. Eckenhoff, J.S. Johansson, Molecular interactions between inhaled anesthetics and proteins, Pharmacological Reviews, 49 (1997) 343-367.
[38] R.Y. Liu, P.J. Loll, R.G. Eckenhoff, Structural basis for high-affinity volatile anesthetic binding in a natural 4-helix bundle protein, Faseb Journal, 19 (2005) 567-576.
[39] S.M. Pop, N. Gupta, A.S. Raza, S.W. Ragsdale, Transcriptional activation of dehalorespiration - Identification of redox-active cysteines regulating dimerization and DNA binding, Journal of Biological Chemistry, 281 (2006) 26382-26390.
[40] A. Memic, M.R. Spaller, How Do Halogen Substituents Contribute to Protein-Binding Interactions? A Thermodynamic Study of Peptide Ligands with Diverse Aryl Halides, Chembiochem, 9 (2008) 2793-2795.
[41] D.A. Kraut, M.J. Churchill, P.E. Dawson, D. Herschlag, Evaluating the Potential for Halogen Bonding in the Oxyanion Hole of Ketosteroid Isomerase Using Unnatural Amino Acid Mutagenesis, Acs Chemical Biology, 4 (2009) 269-273.
[42] W.S. Zou, J. Han, W.J. Jin, Concentration-dependent Br···O halogen bonding between carbon tetrabromide and oxygen-containing organic solvents, Journal of Physical Chemistry A, 113 (2009) 10125-10132.
[43] D. Hauchecorne, B.J. van der Veken, A. Moiana, W.A. Herrebout, The C-Cl···N halogen bond, the weaker relative of the C···I and **C**-Br···N halogen bonds, finally characterized in solution, Chemical Physics, 374 (2010) 30-36.

[44] M.G. Sarwar, B. Dragisic, L.J. Salsberg, C. Gouliaras, M.S. Taylor, Thermodynamics of Halogen Bonding in Solution: Substituent, Structural, and Solvent Effects, Journal of the American Chemical Society, 132 (2010) 1646-1653.
[45] M. Carter, P.S. Ho, Assaying the Energies of Biological Halogen Bonds, Crystal Growth & Design, 11 (2011) 5087-5095.
[46] L.A. Hardegger, B. Kuhn, B. Spinnler, L. Anselm, R. Ecabert, M. Stihle, B. Gsell, R. Thoma, J. Diez, J. Benz, J.-M. Plancher, G. Hartmann, D.W. Banner, W. Haap, F. Diederich, Systematic Investigation of Halogen Bonding in Protein-Ligand Interactions, Angewandte Chemie-International Edition, 50 (2011) 314-318.
[47] J. Poznanski, A. Poznanska, D. Shugar, A Protein Data Bank Survey Reveals Shortening of Intermolecular Hydrogen Bonds in Ligand-Protein Complexes When a Halogenated Ligand Is an H-Bond Donor, Plos One, 9 (2014) e99984.
[48] W. Wang, Y. Okada, H.B. Shi, Y.Q. Wang, T. Okuyama, Structures and aldose reductase inhibitory effects of bromophenols from the red alga Symphyocladia latiuscula, Journal of Natural Products, 68 (2005) 620-622.
[49] M.Z. Hernandes, S.M.T. Cavalcanti, D.R.M. Moreira, W.F. de Azevedo, Jr., A.C. Lima Leite, Halogen Atoms in the Modern Medicinal Chemistry: Hints for the Drug Design, Current Drug Targets, 11 (2010) 303-314.
[50] P.M. Pauletti, L.S. Cintra, C.G. Braguine, A.A. da Silva Filho, M.L. Andrade e Silva, W.R. Cunha, A.H. Januario, Halogenated Indole Alkaloids from Marine Invertebrates, Marine Drugs, 8 (2010) 1526-1549.
[51] F. Meggio, L.A. Pinna, One-thousand-and-one substrates of protein kinase CK2?, Faseb Journal, 17 (2003) 349-368.
[52] M.A. Pagano, J. Bain, Z. Kazimierczuk, S. Sarno, M. Ruzzene, G. Di Maira, M. Elliott, A. Orzeszko, G. Cozza, F. Meggio, L.A. Pinna, The selectivity of inhibitors of protein kinase CK2: an update, Biochemical Journal, 415 (2008) 353-365.
[53] S. Sarno, E. Papinutto, C. Franchin, J. Bain, M. Elliott, F. Meggio, Z. Kazimierczuk, A. Orzeszko, G. Zanotti, R. Battistutta, L.A. Pinna, ATP Site-Directed Inhibitors of Protein Kinase CK2: An Update, Current Topics in Medicinal Chemistry, 11 (2011) 1340-1351.
[54] S. Tawfic, S. Yu, H. Wang, R. Faust, A. Davis, K. Ahmed, Protein kinase CK2 signal in neoplasia, Histology and Histopathology, 16 (2001) 573-582.
[55] K. Niefind, J. Raaf, O.G. Issinger, Protein kinase CK2: From structures to insights, Cellular and Molecular Life Sciences, 66 (2009) 1800-1816.
[56] S. Sarno, H. Reddy, F. Meggio, M. Ruzzene, S.P. Davies, A. Donella-Deana, D. Shugar, L.A. Pinna, Selectivity of 4,5,6,7-tetrabromobenzotriazole, an ATP site-directed inhibitor of protein kinase CK2 ('casein kinase-2'), Febs Letters, 496 (2001) 44-48.
[57] R. Battistutta, E. De Moliner, S. Sarno, G. Zanotti, L.A. Pinna, Structural features underlying selective inhibition of protein kinase CK2 by ATP site-directed tetrabromo-2-benzotriazole, Protein Science, 10 (2001) 2200-2206.
[58] S. Sarno, M. Ruzzene, P. Frascella, M.A. Pagano, F. Meggio, A. Zambon, M. Mazzorana, G. Di Maira, V. Lucchini, L.A. Pinna, Development and exploitation of CK2 inhibitors, Molecular and Cellular Biochemistry, 274 (2005) 69-76.
[59] M.A. Pagano, M. Andrzejewska, M. Ruzzene, S. Sarno, L. Cesaro, J. Bain, M. Elliott, F. Meggio, Z. Kazimierczuk, L.A. Pinna, Optimization of protein kinase CK2 inhibitors derived from 4,5,6,7-tetrabromobenzimidazole, Journal of Medicinal Chemistry, 47 (2004) 6239-6247.
[60] R. Wasik, P. Winska, J. Poznanski, D. Shugar, Synthesis and Physico-Chemical Properties in Aqueous Medium of All Possible Isomeric Bromo Analogues of Benzo-1H-Triazole, Potential Inhibitors of Protein Kinases, Journal of Physical Chemistry B, 116 (2012) 7259-7268.
[61] R. Wasik, P. Winska, J. Poznanski, D. Shugar, Isomeric Mono-, Di-, and Tri-Bromobenzo-1H-Triazoles as Inhibitors of Human Protein Kinase CK2 alpha, Plos One, 7 (2012) e48898.
[62] R. Wasik, M. Lebska, K. Felczak, J. Poznanski, D. Shugar, Relative Role of Halogen Bonds and Hydrophobic Interactions in Inhibition of Human Protein Kinase CK2 alpha by Tetrabromobenzotriazole and Some C(5)-Substituted Analogues, Journal of Physical Chemistry B, 114 (2010) 10601-10611.
[63] M. Winiewska, M. Makowska, P. Maj, M. Wielechowska, M. Bretner, J. Poznański, D. Shugar, Thermodynamic parameters for binding of some halogenated inhibitors of human protein kinase CK2, Biochemical and Biophysical Research Communication, 456 (2015) 282-287.
[64] M.A. Fabian, W.H. Biggs, D.K. Treiber, C.E. Atteridge, M.D. Azimioara, M.G. Benedetti, T.A. Carter, P. Ciceri, P.T. Edeen, M. Floyd, J.M. Ford, M. Galvin, J.L. Gerlach, R.M. Grotzfeld, S. Herrgard, D.E. Insko, M.A. Insko, A.G. Lai, J.M. Lelias, S.A. Mehta, Z.V. Milanov, A.M. Velasco, L.M. Wodicka, H.K. Patel, P.P. Zarrinkar, D.J. Lockhart, A small molecule-kinase interaction map for clinical kinase inhibitors, Nature Biotechnology, 23 (2005) 329-336.

[65] J. Hochscherf, D. Lindenblatt, M. Steinkrtiger, E. Yoo, O. Ulucan, S. Herzig, O.G. Issinger, V. Helms, C. Gotz, I. Neundorf, K. Niefind, M. Pietsch, Development of a high-throughput screening-compatible assay to identify inhibitors of the CK2 alpha/CK2 beta interaction, Analytical Biochemistry, 468 (2015) 4-14.
[66] E. Enkvist, K. Viht, N. Bischoff, J. Vahter, S. Saaver, G. Raidaru, O.-G. Issinger, K. Niefind, A. Uri, A subnanomolar fluorescent probe for protein kinase CK2 interaction studies, Organic & Biomolecular Chemistry, 10 (2012) 8645-8653.
[67] A. Vaasa, I. Viil, E. Enkvist, K. Viht, G. Raidaru, D. Lavogina, A. Uri, High-affinity bisubstrate probe for fluorescence anisotropy binding/displacement assays with protein kinases PKA and ROCK, Analytical Biochemistry, 385 (2009) 85-93.
[68] W. Reindl, K. Strebhardt, T. Berg, A high-throughput assay based on fluorescence polarization for inhibitors of the polo-box domain of polo-like kinase 1, Analytical Biochemistry, 383 (2008) 205-209.
[69] W.X. Zhang, R.X. Wang, D. Wisniewski, A.I. Marcy, P. LoGrasso, J.M. Lisnock, R.T. Cummings, J.E. Thompson, Time-resolved Forster resonance energy transfer assays for the binding of nucleotide and protein substrates to p38 alpha protein kinase, Analytical Biochemistry, 343 (2005) 76-83.
[70] G.A. Romanov, S.N. Lomin, T. Schmuelling, Biochemical characteristics and ligand-binding properties of Arabidopsis cytokinin receptor AHK3 compared to CRE1/AHK4 as revealed by a direct binding assay, Journal of Experimental Botany, 57 (2006) 4051-4058.
[71] E. Chung, D. Henriques, D. Renzoni, M. Zvelebil, J.M. Bradshaw, G. Waksman, C.V. Robinson, J.E. Ladbury, Mass spectrometric and thermodynamic studies reveal the role of water molecules in complexes formed between SH2 domains and tyrosyl phosphopeptides, Structure with Folding & Design, 6 (1998) 1141-1151.
[72] J.D. Taylor, A. Ababou, R.R. Fawaz, C.J. Hobbs, M.A. Williams, J.E. Ladbury, Structure, dynamics, and binding thermodynamics of the v-Src SH2 domain: Implications for drug design, Proteins-Structure Function and Bioinformatics, 73 (2008) 929-940.
[73] I. Lamberto, H. Qin, R. Noberini, L. Premkumar, C. Bourgin, S.J. Riedl, J. Song, E.B. Pasquale, Distinctive binding of three antagonistic peptides to the ephrin-binding pocket of the EphA4 receptor, Biochemical Journal, 445 (2012) 47-56.
[74] T. Klein, J. Tucker, G.A. Holdgate, R.A. Norman, A.L. Breeze, FGFR1 Kinase Inhibitors: Close Regioisomers Adopt Divergent Binding Modes and Display Distinct Biophysical Signatures, Acs Medicinal Chemistry Letters, 5 (2014) 166-171.
[75] E.H. Mashalidis, P. Sledz, S. Lang, C. Abell, A three-stage biophysical screening cascade for fragment-based drug discovery, Nature Protocols, 8 (2013) 2309-2324.
[76] P. Zien, M. Bretner, K. Zastapilo, R. Szyszka, D. Shugar, Selectivity of 4,5,6,7-tetrabromobenzimidazole as an ATP-competitive potent inhibitor of protein kinase CK2 from various sources, Biochemical and Biophysical Research Communications, 306 (2003) 129-133.
[77] J. Shao, J. Chang, C. Chi, Linear and star-shaped pyrazine-containing acene dicarboximides with high electron-affinity, Organic & Biomolecular Chemistry, 10 (2012) 7045-7052.
[78] M. Andrzejewska, M.A. Pagano, F. Meggio, A.M. Brunati, Z. Kazimierczuk, Polyhalogenobenzimidazoles: Synthesis and their inhibitory activity against casein kinases, Bioorganic & Medicinal Chemistry, 11 (2003) 3997-4002.
[79] K. Pilgram, M. Zupan, R. Skiles, Bromination of 2,1,3-benzothiadiazoles, Journal of Heterocyclic Chemistry, 7 (1970) 629-&.
[80] Y. Jin, Y. Kim, S.H. Kim, S. Song, H.Y. Woo, K. Lee, H. Suh, Novel green-light-emitting polymers based on cyclopenta def phenanthrene, Macromolecules, 41 (2008) 5548-5554.
[81] B.A.D. Neto, A.S. Lopes, M. Wust, V.E.U. Costa, G. Ebeling, J. Dupont, Reductive sulfur extrusion reaction of 2,1,3-benzothiadiazole compounds: a new methodology using NaBH4/CoCl2-6H2O as the reducing system, Tetrahedron Letters, 46 (2005) 6843-6846.
[82] T. Kinoshita, Y. Sekiguchi, H. Fukada, T. Nakaniwa, T. Tada, S. Nakamura, K. Kitaura, H. Ohno, Y. Suzuki, A. Hirasawa, I. Nakanishi, G. Tsujimoto, A detailed thermodynamic profile of cyclopentyl and isopropyl derivatives binding to CK2 kinase, Molecular and Cellular Biochemistry, 356 (2011) 97-105.
[83] J. Raaf, K. Klopffleisch, O.G. Issinger, K. Niefind, The catalytic subunit of human protein kinase CK2 structurally deviates from its maize homologue in complex with the nucleotide competitive inhibitor emodin, Journal of Molecular Biology, 377 (2008) 1-8.
[84] J. Raaf, E. Brunstein, O.G. Issinger, K. Niefind, The CK2 alpha/CK2 beta interface of human protein kinase CK2 harbors a binding pocket for small molecules, Chemistry & Biology, 15 (2008) 111-117.
[85] A.D. Ferguson, P.R. Sheth, A.D. Basso, S. Paliwal, K. Gray, T.O. Fischmann, H.V. Le, Structural basis of CX-4945 binding to human protein kinase CK2, Febs Letters, 585 (2011) 104-110.
[86] R. Battistutta, G. Cozza, F. Pierre, E. Papinutto, G. Lolli, S. Sarno, S.E. O'Brien, A. Siddiqui-Jain, M. Haddach, K. Anderes, D.M. Ryckman, F. Meggio, L.A. Pinna, Unprecedented Selectivity and Structural

Determinants of a New Class of Protein Kinase CK2 Inhibitors in Clinical Trials for the Treatment of Cancer, Biochemistry, 50 (2011) 8478-8488.
[87] T. Kinoshita, T. Nakaniwa, Y. Sekiguchi, Y. Sogabe, A. Sakurai, S. Nakamura, I. Nakanishi, Crystal structure of human CK2 alpha at 1.06 angstrom resolution, Journal of Synchrotron Radiation, 20 (2013) 974-979.
[88] G. Cozza, C. Girardi, A. Ranchio, G. Lolli, S. Sarno, A. Orzeszko, Z. Kazimierczuk, R. Battistutta, M. Ruzzene, L.A. Pinna, Cell-permeable dual inhibitors of protein kinases CK2 and PIM-1: structural features and pharmacological potential, Cellular and Molecular Life Sciences, 71 (2014) 3173-3185.
[89] A.S. Konagurthu, J.C. Whisstock, P.J. Stuckey, A.M. Lesk, MUSTANG: A multiple structural alignment algorithm, Proteins-Structure Function and Bioinformatics, 64 (2006) 559-574.
[90] E. Krieger, G. Koraimann, G. Vriend, Increasing the precision of comparative models with YASARA NOVA - a self-parameterizing force field, Proteins-Structure Function and Genetics, 47 (2002) 393-402.
[91] R. Battistutta, M. Mazzorana, L. Cendron, A. Bortolato, S. Sarno, Z. Kazimierczuk, G. Zanotti, S. Moro, L.A. Pinna, The ATP-binding site of protein kinase CK2 holds a positive electrostatic area and conserved water molecules, Chembiochem, 8 (2007) 1804-1809.
[92] D.W. Marquardt, An algorithm for least-squares estimation of nonlinear parameters, Journal of the Society for Industrial and Applied Mathematics, 11 (1963) 431-441.
[93] T. Williams, C. Kelley, Gnuplot 4.5: an interactive plotting program. http://gnuplot.info, 2011.
[94] A. Cooper, M.A. Nutley, A. Wadood, Differential scanning microcalorimetry, Oxford University Press, Oxford, NY, 2000, pp. 287-318.
[95] Y. Cheng, W.H. Prusoff, Relationship between inhibition constant (K_i) and concentration of inhibitor which causes 50 per cent inhibition (I_{50}) of an enzymatic-reaction, Biochemical Pharmacology, 22 (1973) 3099-3108.
[96] K. Niefind, O.G. Issinger, Conformational plasticity of the catalytic subunit of protein kinase CK2 and its consequences for regulation and drug design, Biochimica Et Biophysica Acta-Proteins and Proteomics, 1804 (2010) 484-492.
[97] A. Rastogi, S. Yadav, S.J. Suresh, Note: Extraction of hydrogen bond thermodynamic properties of water from dielectric constant and relaxation time data, Journal of Chemical Physics, 135 (2011).
[98] F.H. Niesen, H. Berglund, M. Vedadi, The use of differential scanning fluorimetry to detect ligand interactions that promote protein stability, Nature Protocols, 2 (2007) 2212-2221.
[99] C.J. Wienken, P. Baaske, U. Rothbauer, D. Braun, S. Duhr, Protein-binding assays in biological liquids using microscale thermophoresis, Nature Communications, 1 (2010).